European Journal of Neurology

european journal of neurology
the official journal of the european academy of neurology

ORIGINAL ARTICLE OPEN ACCESS

Distinctive Progression Patterns of Brain Structural Damage Aid Classification of Frontotemporal Dementia Variants

Edoardo Gioele Spinelli[1,2,3,4] | Francesca Orlandi[1,2,3,4] | Silvia Basaia[1,5] | Francesco Costa[1,4] | Stefano Pisano[1] | Alma Ghirelli[1,2,3,4] | Elisa Canu[1,3,5] | Veronica Castelnovo[1,3] | Elisa Sibilla[1,3] | Giordano Cecchetti[1,2,3,6] | Francesca Caso[2,3] | Giuseppe Magnani[2,3] | Paola Caroppo[7] | Sara Prioni[7] | Cristina Villa[7] | Lucio Tremolizzo[8] | Ildebrando Appollonio[8] | Federico Verde[9] | Nicola Ticozzi[9,10] | Vincenzo Silani[9,10] | Massimo Filippi[1,2,3,4,5,6,11] | Federica Agosta[1,2,3,4,5]

[1]Neuroimaging Research Unit, Division of Neuroscience, IRCCS San Raffaele Scientific Institute, Milan, Italy | [2]Neurology Unit, IRCCS San Raffaele Scientific Institute, Milan, Italy | [3]Center for Alzheimer's Disease and Related Disorders (CARD), IRCCS San Raffaele Scientific Institute, Milan, Italy | [4]Vita-Salute San Raffaele University, Milan, Italy | [5]Neurotech Hub, Vita-Salute San Raffaele University, Milan, Italy | [6]Neurophysiology Service, IRCCS San Raffaele Scientific Institute, Milan, Italy | [7]Unit of Neurology 5-Neuropathology, Fondazione IRCCS Istituto Neurologico Carlo Besta, Milan, Italy | [8]Neurology Unit, "San Gerardo" Hospital and University of Milano-Bicocca, Monza, Italy | [9]Department of Neurology and Laboratory of Neuroscience, IRCCS Istituto Auxologico Italiano, Milano, Italy | [10]"Dino Ferrari" Center, Department of Pathophysiology and Transplantation, Università Degli Studi di Milano, Milan, Italy | [11]Neurorehabilitation Unit, IRCCS San Raffaele Scientific Institute, Milan, Italy

Correspondence: Federica Agosta (agosta.federica@hsr.it)

Received: 30 April 2025 | **Revised:** 16 June 2025 | **Accepted:** 19 June 2025

Funding: Next Generation EU/National Recovery and Resilience Plan, Investment PE8-Project Age-It: "Ageing Well in an Ageing Society". Edoardo Gioele Spinelli was co-financed by the Next Generation EU [DM 1557 11.10.2022]. The views and opinions expressed are only those of the authors and do not necessarily reflect those of the European Union or the European Commission. Neither the European Union nor the European Commission can be held responsible for them. European Research Council (StG-2016_714388_NeuroTRACK). Foundation Research on Alzheimer Disease.

Keywords: frontotemporal dementia | longitudinal atrophy progression | neuroimaging | principal component analysis | support vector machine

ABSTRACT

Background: Frontotemporal dementia (FTD) encompasses diverse clinical phenotypes, primarily characterized by behavioral and/or language dysfunction. A newly characterized variant, semantic behavioral variant FTD (sbvFTD), exhibits predominant right temporal atrophy with features bridging behavioral variant FTD (bvFTD) and semantic variant primary progressive aphasia (svPPA). This study investigates the longitudinal structural MRI correlates of these FTD variants, focusing on cortical and subcortical structural damage to aid differential diagnosis and prognosis.

Methods: Seventy-one FTD patients (bvFTD = 45, sbvFTD = 11, svPPA = 15) and 37 healthy controls participated in a prospective study involving up to 24 months of serial neurological, neuropsychological, and 3T MRI assessments. Cortical thickness and subcortical/cerebellar volumes were analyzed with linear mixed-effect models. Support vector machine (SVM) models were used to classify subjects using baseline and longitudinal patterns of structural damage.

Results: At baseline, sbvFTD showed right-predominant temporal pole involvement associated with significant right frontal atrophy. Longitudinally, bvFTD showed widespread bilateral cortical and basal ganglia damage, svPPA demonstrated steady temporal lobe progression, and sbvFTD progressed primarily in left temporal and frontal regions with limited right hemisphere involvement. Baseline cortical thickness of frontal regions predicted subsequent functional decline in bvFTD and sbvFTD. A multiclass SVM model provided a good diagnostic classification accuracy, with similar results when using baseline data only (82%) and adding longitudinal data (83%).

Conclusions: This study delineates the unique structural MRI features and progression of FTD variants, highlighting sbvFTD as a distinct entity with early extra-temporal involvement. These findings support the development of diagnostic and prognostic tools leveraging neuroimaging biomarkers.

1 | Introduction

Frontotemporal dementia (FTD) poses a diagnostic challenge due to overlapping clinical presentations and heterogeneous neuropathological substrates [1]. Novel diagnostic entities and updated classification criteria help clinicians navigate this complex spectrum [2]. It is now recognized that diagnostic accuracy can be significantly improved by combining clinical knowledge with quantitative measures of pathology, including advanced neuroimaging [3]. Extensive research has been conducted in this area, bringing about outstanding progress in the understanding of the anatomical and functional correlates of the FTD syndromes.

In recent years, it has become clear that atrophy in the non-dominant anterior temporal lobe presents with a unique clinical profile that might not fit the current diagnostic criteria for semantic variant primary progressive aphasia (svPPA) [4], nor those for behavioral variant of FTD (bvFTD) [5]. Recent efforts have been made to provide a systematic overview of this condition, characterized by early behavioral alterations and socioemotional semantic deficits [6, 7] and variably defined as 'right temporal variant FTD', 'FTD with right anterior temporal predominance' [6], or 'semantic behavioral variant FTD (sbvFTD)' [8].

This study aimed to assess and compare the longitudinal structural MRI correlates of bvFTD, svPPA, and sbvFTD, reinforcing the view of sbvFTD as a distinct clinicopathological entity. The study aims to identify consistent imaging biomarkers to improve the accuracy of FTD diagnosis, enhance prognostic assessments, and support the proper classification of patients for inclusion in clinical trials evaluating disease-modifying treatments.

2 | Methods

Participants or their caregivers provided written informed consent, and the study received approval from the local ethics committee in accordance with the Declaration of Helsinki.

2.1 | Participants

For this prospective, multicenter study, participants were selected among 283 patients with a suspected diagnosis of the FTD/motor neuron disease spectrum who were referred to four specialized clinics in Lombardy, Italy, and underwent brain MRI on a 3 Tesla scanner between March 2017 and July 2022. Of these, 65 patients met the diagnostic criteria of bvFTD [5], 25 those of svPPA [4], and 15 were classified as sbvFTD according to the proposed guidelines [8]. Two patients with a bvFTD diagnosis and concurrent motor neuron disease signs were excluded to avoid confounding effects. Patients underwent periodic follow-up visits including the same assessments approximately on a 6-month basis. Only patients with at least two good-quality longitudinal MRI scans were included. Exclusion criteria included significant medical, psychiatric, or neurological conditions and widespread cerebrovascular disease. Ultimately, 45 bvFTD, 15 svPPA, and 11 sbvFTD patients underwent further analyses (Figure S1 and Table 1). Of these, 37 underwent cerebrospinal fluid analysis (24 bvFTD, 5 svPPA and 8 sbvFTD), confirming no Alzheimer-like biomarker signature, as indicated by a pTau/Aß42 ratio >0.13 [9]. Genetic testing results for *C9orf72*, *GRN*, and *MAPT* genes were available for all but three subjects (2 bvFTD, 1 sbvFTD). Thirty-seven healthy controls were recruited among patients' spouses or by word of mouth. All subjects were followed up on a 6-month basis for a period of up to 24 months (median follow-up time = 16.9 months; mean number of MRI scans = 3.24). Demographics and clinical features of patients and controls at baseline are shown in Table 1 (see Data S1 for details). Baseline clinical data of the present longitudinal cohort (100%) were previously reported [7].

2.2 | MRI Analysis

Participants underwent serial brain MRI scans on the same 3 T scanner (Philips Medical Systems, Best, the Netherlands) [10]. The protocol is detailed in the Data S1.

2.2.1 | Cortical Thickness Analysis

Cortical reconstruction and estimation of cortical thickness were performed on the 3D T1-weighted TFE images using FreeSurfer, version 5.3 [11]. The serial MRI images from each subject were processed with the FreeSurfer longitudinal stream [12]. Further methodological details are provided in the Data S1.

2.2.2 | Subcortical, Hippocampal and Cerebellar Volume Analysis

Volumes of the bilateral caudate, pallidum, putamen, thalamus, and hippocampus were obtained using the FIRST tool in FSL [13]. For extraction of cerebellar volumes, the SUIT toolbox was used [14–16]. Subcortical gray matter (GM) volumes and cerebellar volumes were multiplied by the normalization factor derived from SIENAx to correct for individual head size [17].

For both cortical thickness and volumetric analyses, visual inspection of segmentation outputs was performed to ensure the accuracy of the results.

2.3 | Statistical Analysis

2.3.1 | Demographic, Clinical and Neuropsychological Data

Demographic and clinical parameters were compared using ANOVA models, while categorical variables were analyzed with

TABLE 1 | Demographics and clinical features of FTD patients and healthy controls at baseline.

	bvFTD ($n=45$)	sbvFTD ($n=11$)	svPPA ($n=15$)	HC ($n=37$)	p.
Age	65.1 ± 8.1 (36.5–79.8)	61.6 ± 8.7 (48.4–77.1)	64.2 ± 9.8 (42.1–75.3)	61.5 ± 9.3 (40.7–77.8)	0.23
Sex (M/F)	29/16	6/5	7/8	15/22	0.12
Education (years)	10.5 ± 3.5 (3–19)	10.3 ± 4.6 (5–21)	13.7 ± 3.3 (5–17)	12.6 ± 4.1 (5–21)	**0.03**
Disease duration (years)	3.2 ± 1.8 (0.9–8.9)	2.5 ± 1.27 (0.1–4.8)	5.6 ± 4.6 (1.1–20.2)	—	**0.005**[a, b]
ADL (/6)	5.1 ± 1.5 (1–6)	5.7 ± 0.7 (4–6)	5.6 ± 0.7 (4–6)	—	0.21
IADL (/8)	6.7 ± 2.3 (0–8)	6.6 ± 2.5 (0–8)	6.9 ± 2.2 (0–8)	—	0.97
CDR	1.4 ± 1.3 (0–6)	1 ± 0.8 (0–2)	1 ± 0.7 (0–2)	—	0.72
CDR-sb	6.3 ± 4.7 (1–17)	5.0 ± 4.6 (1–14)	6.8 ± 2.9 (2–11)	—	0.75
CDR plus NACC FTLD-sb	8.4 ± 6.3 (1–23)	7.6 ± 6.8 (3–18)	5.9 ± 4.8 (1–14)	—	0.60
MMSE (/30)	23 ± 6.2 (6–30)	26.6 ± 2.6 (22–30)	20.9 ± 8.1 (5–30)	29.2 ± 0.9 (27–30)	**< 0.001**[b, c, d]
FAB (/18)	10.9 ± 4 (2–17)	12.9 ± 3.3 (5–16)	12.1 ± 5.1 (0–17)	—	0.23
NPI (/144)	29.3 ± 19.6 (3–74)	21.1 ± 23 (4–76)	20.2 ± 14.9 (3–46)	—	0.26
CSF amyloid β42 (ng/L)	885.1 ± 319.4 (528–1619)	760.8 ± 216.8 (492–1123)	773.4 ± 268.2 (430–1091)	—	0.51
CSF total tau (ng/L)	330.3 ± 161.9 (95–451)	271.4 ± 106.7 (130–484)	258.6 ± 77.3 (175–356)	—	0.44
CSF p181-tau (ng/L)	40.18 ± 17.2 (15–65)	32.1 ± 7.1 (21–39)	29.3 ± 6.7 (23–38)	—	0.32
Genetic mutation status (n, % positive)	12 (26%)				
GRN (9), c9orf72 (2), MAPT (1)	2 (18%) c9orf72 (1)				
MAPT (1)	1 (6%) MAPT (1)				

Note: Mean ± standard deviation (min. value–max. value) are reported. p values refer to ANOVA model, followed by Bonferroni post hoc test for multiple comparisons (number of comparisons = 14), or Fisher's exact test, as appropriate. a = $p < 0.05$ bvFTD vs. svPPA; b = $p < 0.05$ sbvFTD vs. svPPA; c = $p < 0.05$ bvFTD vs. HC; d = $p < 0.05$ svPPA vs. HC.

Abbreviations: ADL = activities of daily living, bvFTD = behavioral variant frontotemporal dementia, CDR = clinical dementia rating, CDR plus NACC FTLD = clinical dementia rating for frontotemporal dementia, CDR-sb = clinical dementia rating sum of boxes, CSF = cerebrospinal fluid, HC = Healthy Controls, IADL = instrumental activities of daily living, NPI = neuropsychiatric inventory, sbvFTD = semantic behavioral variant FTD, svPPA = semantic variant primary progressive aphasia. Bold is for significant values.

chi-square tests. Neuropsychological scores at baseline were assessed with ANCOVA models adjusted for age, sex, education, and CDR plus NACC FTLD. Pairwise post hoc comparisons were Bonferroni-corrected for multiple comparisons (i.e., number of variables), with statistical significance set at $p < 0.05/m$, where m represents the number of comparisons performed. Longitudinal changes in CDR plus NACC FTLD scores and neuropsychological variables were analyzed using linear mixed effects models, with age, sex, education, baseline CDR plus NACC FTLD, and follow-up time as covariates. Analyses were performed in R Software (v4.3.2).

2.3.2 | Cross-Sectional and Longitudinal GM Structural Analysis

Baseline cortical thickness and subcortical, hippocampal, and cerebellar volumes were compared using ANCOVA models adjusted for age, sex, education, and CDR plus NACC FTLD. Pairwise group comparisons were Bonferroni-corrected for multiple comparisons. Longitudinal changes in these measures were evaluated with linear mixed effects models, incorporating visit timepoint, age, sex, education, baseline CDR plus NACC FTLD, and follow-up time as predictors. Pairwise comparisons of estimated trends were Bonferroni-corrected for multiple comparisons. Analyses were performed in R Software (v4.3.2). For descriptive purposes, cross-sectional and longitudinal vertex-by-vertex analyses were also performed in FreeSurfer, FDR-corrected for multiple comparisons (see Data S1).

2.3.3 | MRI Predictors of Clinical Progression

Baseline GM values of FTD patients were normalized relative to controls and input into linear regression models to assess their utility to predict annualized changes in CDR plus NACC FTLD

(%). Log-transformed CDR plus NACC FTLD values were used in linear mixed effects models, and regression coefficients were back-transformed to express predictors' effects as percentage change. Analyses were performed in R Software (v4.3.2).

2.3.4 | Classification Models

To compare the utility of cross-sectional vs. longitudinal atrophy patterns for differential diagnosis of FTD variants, we used a pipeline that has been previously described [18] applying unsupervised and supervised machine learning (ML). Baseline cortical thickness and subcortical volumes were input into a support vector machine (SVM) classifier after principal component analysis (PCA) reduced input feature complexity. A similar approach was applied for longitudinal classification using baseline and follow-up measures. Regional weights for the first components were extracted to visually verify the consistency with disease-specific patterns (Figure S2). Classification performance was assessed with stratified 10-fold cross-validation, and SVM hyperparameters were optimized via Grid Search. Analyses were conducted in Python using scikit-learn.

3 | Results

3.1 | Clinical, Genetic and Neuropsychological Findings

3.1.1 | Baseline Analysis

At baseline, the study groups were comparable in age and sex (Table 1), though bvFTD patients had slightly lower education levels compared to controls and svPPA. Disease duration was longer in svPPA patients than in other patient groups. CDR plus NACC FTLD scores at baseline were similar across FTD groups. Genetic analysis revealed pathogenic variants in 12 bvFTD patients (*GRN* = 9, *C9orf72* = 2, *MAPT* = 1), 2 sbvFTD patients (*C9orf72* = 1, *MAPT* = 1), and 1 svPPA patient (*MAPT*).

Neuropsychological assessments (Table S1) revealed significant cognitive deficits across all FTD groups compared to healthy controls in memory, attention, executive functions, language, and social cognition. bvFTD patients exhibited pronounced executive and visuospatial deficits, svPPA patients were severely impaired in naming and comprehension, and sbvFTD patients had milder language impairments than svPPA.

3.1.2 | Longitudinal Analysis

All FTD groups showed cognitive and functional decline over time, with worsening CDR plus NACC FTLD, MMSE, and several measures of memory, executive, language, and behavioral impairment (Table S2). The rate of decline in CDR plus NACC FTLD scores was comparable across FTD groups.

Of note, patients with sbvFTD showed a significant decline in measures of both attentive-executive (i.e., Trail Making Test, attentive matrices, semantic fluency) and linguistic functions (i.e., token test).

3.2 | Cortical Thickness

3.2.1 | Baseline Analysis

Compared to healthy controls, bvFTD patients displayed significant cortical thinning in almost all right frontal and temporal regions, left superior frontal and orbitofrontal cortices, and right supramarginal gyrus (Figures 1a, S3, Tables S3, S4). sbvFTD patients exhibited severe thinning in the right hemisphere, including temporal, frontal (orbitofrontal, superior frontal), inferior parietal, and insular regions, along with the left temporal regions (temporal pole, entorhinal, inferior temporal) (Figure 1b). svPPA patients showed bilateral temporal thinning with left-sided predominance, affecting the bilateral insula (left > right), left orbitofrontal, and left lateral occipital regions (Figure 1c).

Compared to bvFTD, sbvFTD demonstrated greater thinning in the right temporal regions and left fusiform gyrus (Figure 1d). svPPA showed greater thinning than bvFTD in the left hemisphere, including the entorhinal cortex, fusiform gyrus, temporal regions, and frontal pole, whereas bvFTD showed greater thinning in the right pars orbitalis (Figure 1e). Compared to svPPA, sbvFTD had reduced cortical thickness in the right fusiform and temporal gyri, while svPPA showed more extensive thinning of the left fusiform gyrus, temporal gyri, temporal pole, insula, and medial orbitofrontal cortex (Figure 1f).

3.2.2 | Longitudinal Analysis

Compared to healthy controls, bvFTD showed faster progression of cortical thinning over time, predominantly in the right temporal lobe (entorhinal cortex, fusiform gyrus, inferior and middle temporal gyri), as well as in right frontal and bilateral parietal regions (Figure 2a, Figure S4, Tables S7, S8). sbvFTD exhibited more rapid progression in bilateral temporal lobes with a left-sided predominance (Figure 2b). sbvFTD also showed greater progression in the left lateral orbitofrontal cortex and left supramarginal gyrus. svPPA displayed accelerated thinning of bilateral temporal lobes with right-sided predominance, involving the fusiform gyrus, parahippocampal cortex, and temporal pole (Figure 2c).

Comparing FTD variants, sbvFTD showed more rapid progression in the left temporal lobe compared to bvFTD and in the left entorhinal cortex, fusiform gyrus, and temporal pole compared to svPPA (Figure 2d,e, Table S7). No significant differences were observed between bvFTD and svPPA. Patients with bvFTD or svPPA did not display regions with greater progression compared to sbvFTD.

3.3 | Subcortical and Hippocampal Volumes

3.3.1 | Baseline Analysis

At baseline, bvFTD patients showed significantly reduced volumes in the bilateral caudate nuclei, putamina, hippocampi, and right thalamus compared to controls (Figure 3a and Table S5).

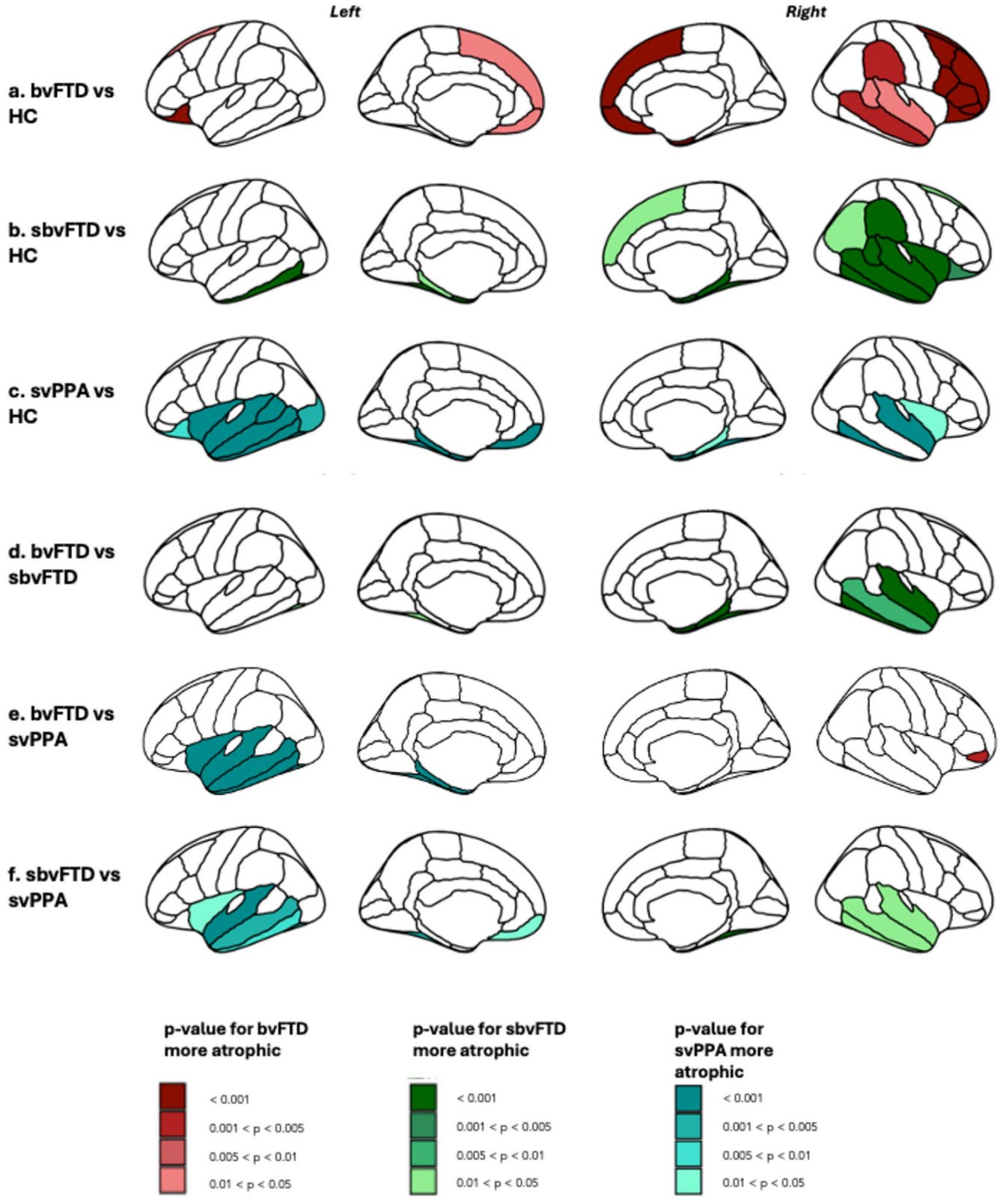

FIGURE 1 | Baseline patterns of cortical thinning in FTD variants. Only significant comparisons are reported ($p < 0.05$, Bonferroni correction). BvFTD = behavioral variant frontotemporal dementia, HC = healthy control, sbvFTD = semantic behavioral variant frontotemporal dementia, svPPA = semantic variant primary progressive aphasia.

sbvFTD patients exhibited lower volumes in the right putamen, right thalamus, and bilateral hippocampi (Figure 3b), while svPPA patients displayed reduced volumes in the left putamen and left hippocampus (Figure 3c).

In comparisons among FTD variants, bvFTD patients had smaller left caudate volumes compared to sbvFTD (Figure 3d) and reduced right caudate and thalamic volumes compared to svPPA (Figure 3e). No regions had smaller volumes in sbvFTD or

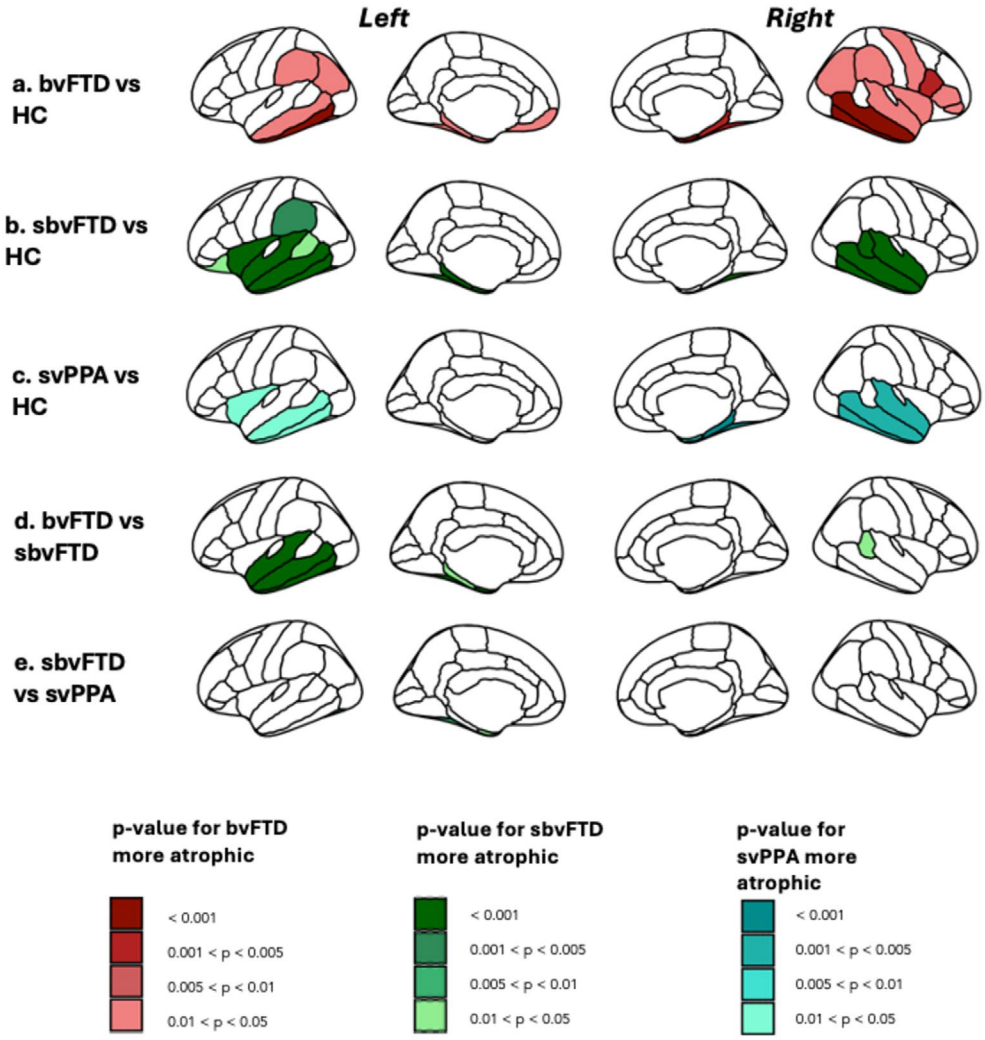

FIGURE 2 | Longitudinal progression patterns of cortical thinning in FTD variants. Only significant comparisons are reported ($p < 0.05$, Bonferroni correction). BvFTD = behavioral variant frontotemporal dementia, HC = healthy control, sbvFTD = semantic behavioral variant frontotemporal dementia, svPPA = semantic variant primary progressive aphasia.

svPPA compared to bvFTD. sbvFTD patients showed decreased right hippocampal volume relative to svPPA, while svPPA had reduced left putamen volume compared to sbvFTD (Figure 3f).

3.3.2 | Longitudinal Analysis

Compared to healthy controls, bvFTD patients showed faster atrophy progression in the bilateral pallidum, putamen, and thalamus (Figure 4a and Table S9). sbvFTD demonstrated accelerated atrophy in the bilateral putamen and thalamus, left hippocampus, left pallidum, and right caudate (Figure 4b). svPPA showed more rapid atrophy in the left putamen and right hippocampus (Figure 4c). No significant differences in the rate of subcortical or hippocampal atrophy progression were found between FTD subtypes.

3.4 | Cerebellar Volumes

No significant differences were found among study groups for either the cross-sectional (Table S6) or longitudinal analyses of cerebellar volumes (Table S10).

3.5 | Predictors of Clinical Progression Over Time

In bvFTD, baseline cortical thickness in frontal regions such as the orbitofrontal cortex, inferior frontal gyrus, and superior frontal cortex significantly predicted progression of CDR plus NACC FTLD scores over time (Figure 5a and Table S11). In sbvFTD, predictive regions included both left and right frontal areas, such as the orbitofrontal cortex, anterior cingulate, and superior frontal cortex (Figure 5b). No cortical or subcortical regions were significant predictors in svPPA, and subcortical, hippocampal, and cerebellar volumes did not predict progression in any group.

3.6 | ML Classification Analysis

The SVM models using cross-sectional MRI data achieved excellent accuracy in distinguishing healthy controls from FTD variants (90%–100%), differentiating between FTD variants (80%–97%), and classifying all groups (82.2%) (Table 2). When incorporating both cross-sectional and longitudinal MRI data, classification accuracy remained high (82%–100%), with the

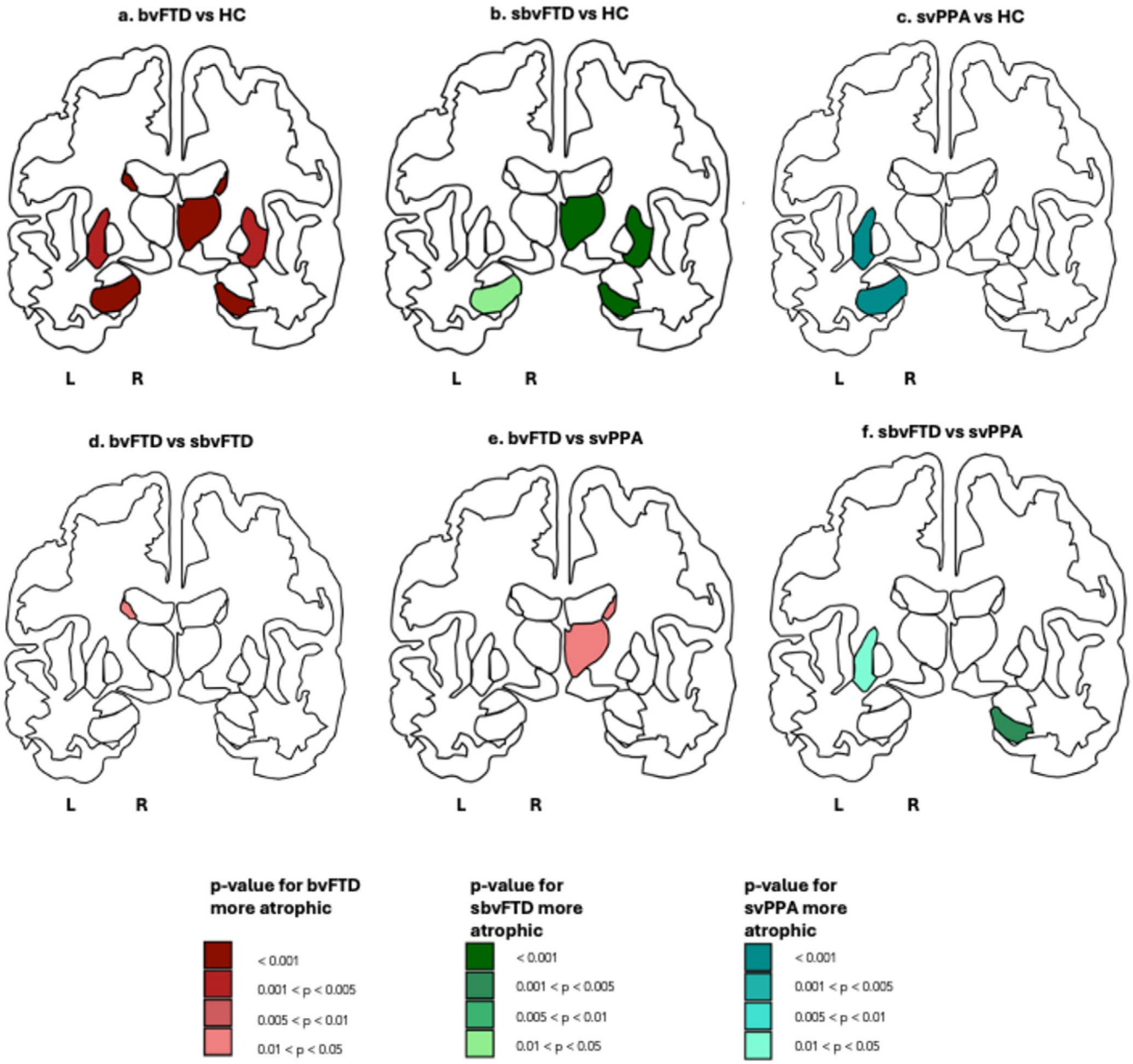

FIGURE 3 | Baseline patterns of subcortical and hippocampal volumetric alterations in FTD variants. Only significant comparisons are reported ($p < 0.05$, Bonferroni correction). BvFTD = behavioral variant frontotemporal dementia, HC = healthy control, sbvFTD = semantic behavioral variant frontotemporal dementia, svPPA = semantic variant primary progressive aphasia.

quaternary model for classification among all study groups improving slightly to 83%.

4 | Discussion

In this longitudinal study, we described the clinical and structural brain MRI trajectories of three variants of the FTD spectrum. For each variant, we delineated baseline patterns of GM loss and estimated longitudinal patterns of structural damage spread over time, highlighting measures with a significant importance for prognostic prediction of disease progression and for differential diagnosis among these partially overlapping clinical variants. Besides the well-recognized bvFTD and svPPA, our cohort also included patients with a clinical diagnosis of sbvFTD [8]. Our study provides a contribution to the ongoing scientific effort aimed at precisely defining the distinctive neuroanatomical and clinical characteristics of sbvFTD.

The baseline cognitive profiles of FTD patients were consistent with the definition criteria of bvFTD and svPPA [4, 5] and previous studies on sbvFTD [6–8] as reported in the recent cross-sectional study describing clinical and neuropsychological findings of the same cohort [7]. FTD patient groups exhibited similar baseline global disease severity, sharing multidomain cognitive deficits. However, sbvFTD patients showed relative preservation in verbal working memory, selective

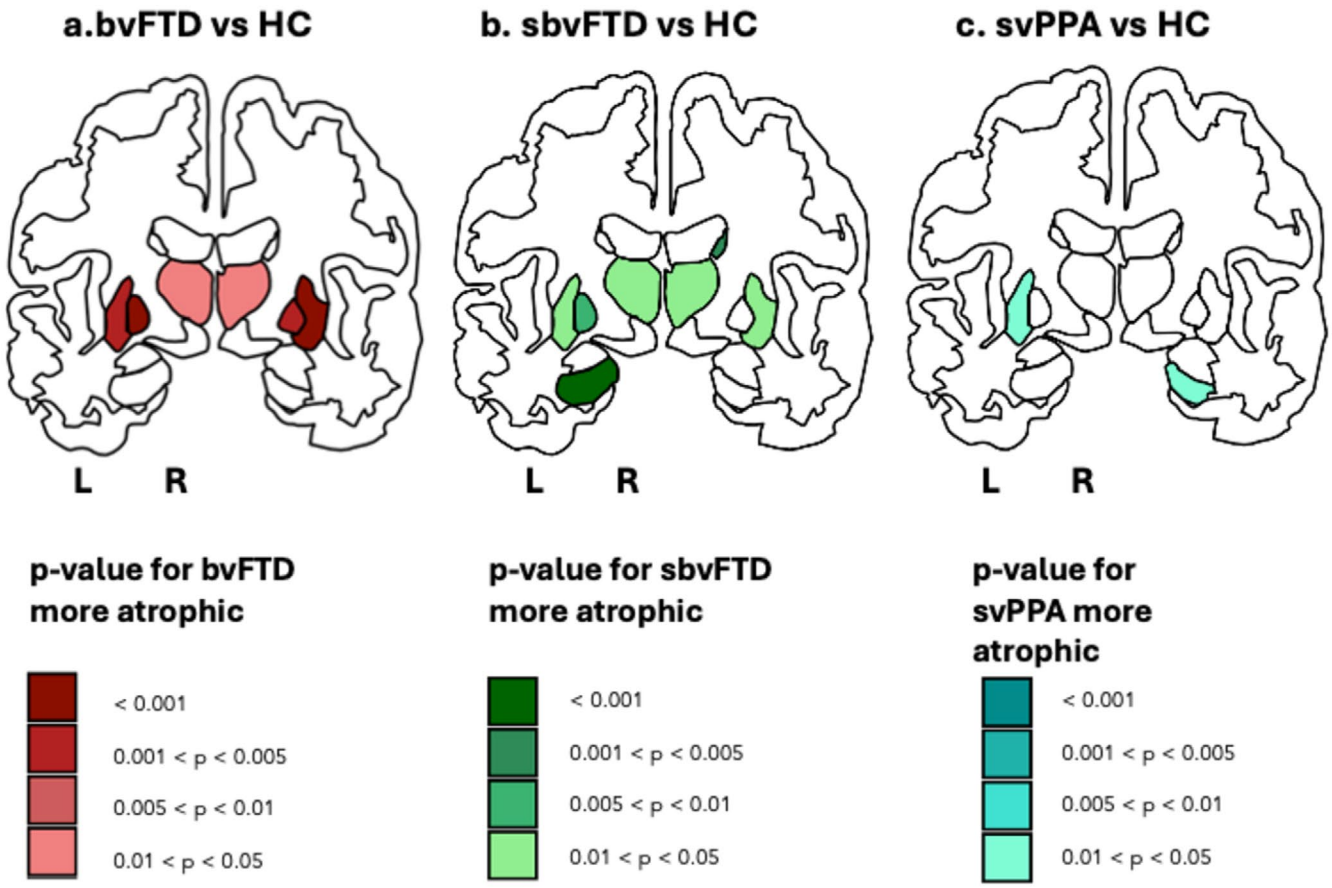

FIGURE 4 | Longitudinal progression patterns of subcortical and hippocampal volumetric alterations in FTD variants. Only significant comparisons are reported ($p < 0.05$, Bonferroni correction). BvFTD = behavioral variant frontotemporal dementia, HC = healthy control, sbvFTD = semantic behavioral variant frontotemporal dementia, svPPA = semantic variant primary progressive aphasia.

attention, confrontation naming, and language comprehension. Longitudinally, all groups demonstrated comparable declines in CDR plus NACC FTLD and behavioral measures. Specifically, sbvFTD patients experienced combined declines in attentive/executive and language functions, while bvFTD showed generalized cognitive deterioration and svPPA exhibited isolated linguistic decline.

The neuroanatomical patterns of GM structural damage in the three FTD variants aligned with their respective clinical profiles. At baseline, bvFTD patients showed widespread cortical atrophy, primarily in the frontal lobes and, to a lesser extent, the temporal lobes [19–21]. Subcortical structures, including striatal and thalamic regions, were also substantially affected, consistent with studies identifying extensive subcortical damage in early bvFTD [22–25]. svPPA exhibited a more confined pattern of structural damage, with marked left-hemispheric temporal cortical, hippocampal, and putaminal damage and only subtle involvement of the left orbitofrontal cortex and contralateral temporal regions [20, 26, 27]. The sbvFTD cohort showed predominant cortical thinning in the right temporal lobe, with additional involvement of the ipsilateral ventral frontal and lateral parietal cortices and contralateral temporal regions. This distribution resembles svPPA but includes right-predominant frontoparietal cortical thinning. Frontal shift of atrophy has already been suggested as an early feature of sbvFTD [28] that is not typically observed in svPPA and is consistent with the greater degree of attentive/executive deficits observed in sbvFTD patients of our cohort. Although we did not observe significant cerebellar involvement in our sample, previous studies have reported cerebellar gray and white matter alterations across FTD phenotypes [21, 29, 30]. Such discrepancies may reflect differences in methodology or the possibility that cerebellar changes are more subtle than cortical and subcortical alterations.

The longitudinal MRI analysis revealed key insights into disease progression across different FTD variants. Regions less affected at baseline showed more rapid progression of GM loss, while heavily damaged areas progressed slower, suggesting a "catch-up" phenomenon as severely affected regions approach a degeneration plateau. In bvFTD—the variant showing the greatest degree of GM loss progression [20, 31]—the greatest GM loss occurred in the bilateral temporal lobes, with steady degeneration in the right frontal and bilateral parietal lobes, and extended subcortical damage to the bilateral pallidum and left thalamus. By contrast, svPPA showed the lesser degree of GM damage progression, mostly concentrated within the right temporal cortical regions. sbvFTD showed a similar bilateral progression within the temporal lobes, although the asymmetry for a greater progression to the contralateral (left) hemisphere was less evident as compared to svPPA, and some extra-temporal regions were also involved. Additionally, sbvFTD showed a widespread subcortical atrophy pattern absent in svPPA, resembling

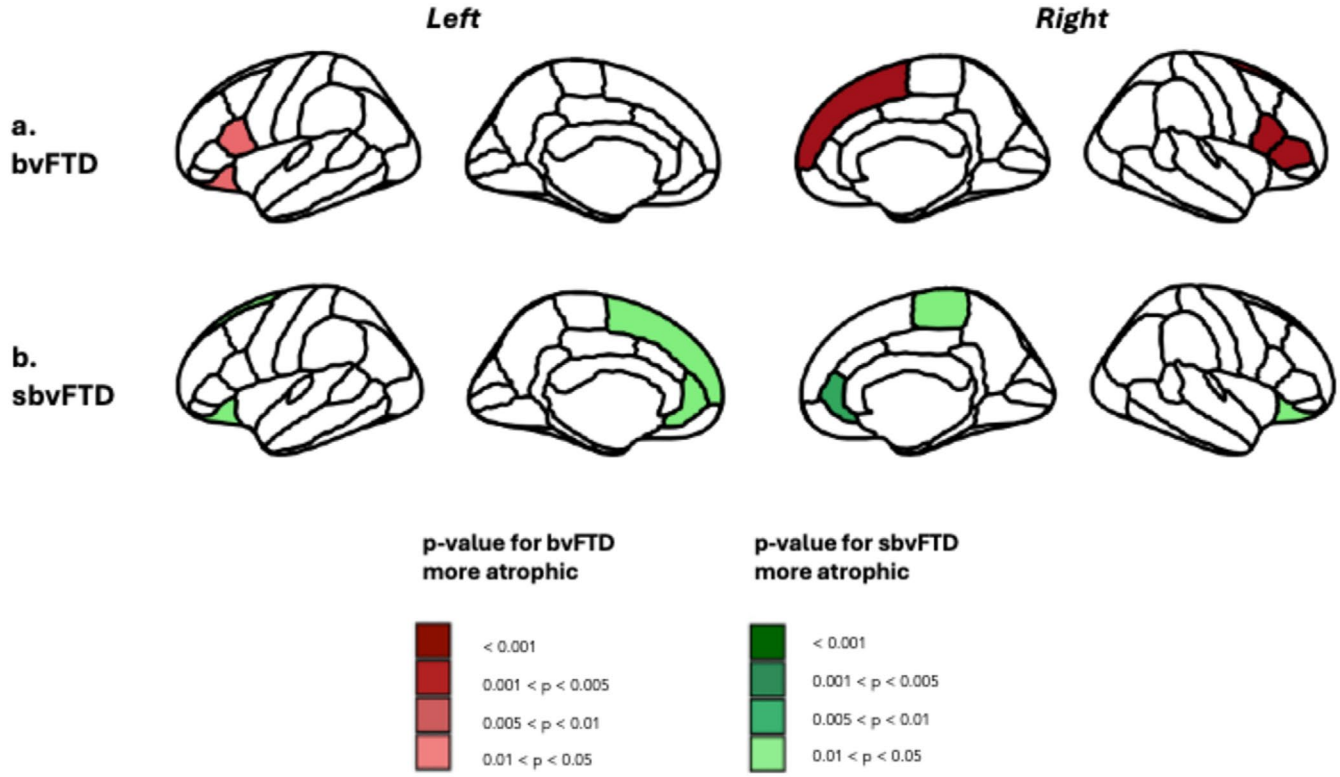

FIGURE 5 | Prognostically relevant gray matter regions in FTD variants. Patterns of regional volumes at baseline predicting CDR plus NACC FTLD percentage change over time in FTD patient groups. Only significant comparisons are reported ($p < 0.05$, uncorrected).

TABLE 2 | Accuracy of SVM classification models using baseline vs. longitudinal GM atrophy measures.

Groups	Accuracy of model with baseline data	SD	Accuracy of model with longitudinal data	SD
HC vs. bvFTD	0.887	0.088	0.893	0.054
HC vs. sbvFTD	1.00	0	1.00	0
HC vs. svPPA	0.98	0.06	0.98	0.06
bvFTD vs. sbvFTD	0.9	0.133	0.91	0.117
bvFTD vs. svPPA	0.95	0.076	0.913	0.115
sbvFTD vs. svPPA	0.95	0.15	0.95	0.15
bvFTD vs. sbvFTD vs. svPPA	0.84	0.135	0.826	0.14
HC vs. bvFTD vs. sbvFTD vs. svPPA	0.822	0.083	0.83	0.11

Abbreviations: bvFTD = behavioral variant frontotemporal dementia, HC = healthy control, sbvFTD = semantic behavioral variant frontotemporal dementia, svPPA = semantic variant primary progressive aphasia, SD = standard deviation.

bvFTD instead. Given that tau pathology has been associated with significant subcortical atrophy in bvFTD [24], this finding in sbvFTD may indicate neuropathologic heterogeneity. In fact, a recent neuropathological case series has shown that up to 25% of sbvFTD cases were accompanied by FTLD-tau pathology [32], unlike svPPA, which is overwhelmingly linked to FTLD-TDP type C pathology [33]. However, without *post-mortem* neuropathological data, this hypothesis remains speculative.

Summarizing, the present structural brain MRI findings describe: (i) a widespread cortical (frontal greater than temporal) and subcortical damage in bvFTD, which progressed mostly through extra-frontal regions; (ii) a localized involvement of the temporal cortical brain regions in svPPA, with early involvement of the left hemisphere followed by progression to the contralateral homologous regions; (iii) sbvFTD showing early—though mild—involvement of extra-right temporal regions (i.e., frontal and parietal cortical and subcortical areas), which kept degenerating over time, in addition to the progression within the temporal lobe resembling a "mirror" representation of svPPA.

Consistent with the hypothesis that the involvement of extra-temporal brain networks in sbvFTD might be a key pathogenic event in the progression of this variant, accelerating its disease

course, the regions predicting a more rapid decline of CDR plus NACC FTLD were identified in fronto-cingulate regions more classically involved in bvFTD [34]. By contrast, svPPA did not show any significant region where GM loss had a prognostically relevant role, supporting the idea of a more homogeneous disease course and a steady progression within temporal hubs. However, such preliminary hypotheses warrant demonstration using network-based connectivity analyses.

Our SVM classification analysis achieved relatively high accuracy in distinguishing FTD variants from healthy controls and from each other using baseline data, as compared with most prior models, which primarily focused on bvFTD without discerning among different FTD phenotypes [18, 35]. These findings suggest that early patterns of brain damage, as described by structural MRI in both cortical and subcortical regions, might support the clinical diagnosis in cases when the differential may not be well defined on clinical grounds only. Including longitudinal data in the SVM models provided minimal accuracy improvement, aligning with observations of slower progression in initially degenerated areas, indicating a potential "ceiling effect." This suggests that while baseline differences are particularly relevant for distinguishing FTD variants, the later-stage convergence of structural damage across variants could limit their diagnostic utility over time [36, 37].

The strengths of this study include a long follow-up of subjects, which helped in the estimation of reliable progression trends, and the inclusion of a group of patients with sbvFTD, a variant still lacking reports of longitudinal atrophy progression. In this context, compared to the more widespread degeneration in bvFTD and the focal temporal involvement in svPPA, sbvFTD showed an intermediate pattern with right-predominant temporal atrophy extending into frontal, parietal, and subcortical regions—mirroring svPPA anatomically but aligning with bvFTD in its progression and prognostic markers.

Some limitations should be acknowledged. First, internal cross-validation might limit the generalizability of our ML algorithms, and robust validation would require testing their classification accuracy on external cohorts. Second, we acknowledge the limitations related to the small sample size and the potential risk of overfitting—especially for the svPPA and sbvFTD groups. Third, no *post-mortem* neuropathological diagnosis was available for the present cohort. Fourth, in order to limit the number of comparisons—which were already substantial—we did not examine thalamic subfields, although recent literature suggests that focal, nucleus-specific thalamic atrophy may better reflect the clinical heterogeneity of FTD phenotypes [38]. Finally, while we focused on GM changes using T1-weighted MRI, the inclusion of additional imaging modalities—such as diffusion tensor imaging—is expected to provide key complementary information in studies assessing trajectories of structural damage in FTD [39].

All this considered, our findings provide an extensive account of the neuroanatomical correlates of disease progression in FTD variants. We characterized variant-specific patterns of brain structural damage at baseline as well as longitudinal trends of progression over time. While further validation in larger, multisite cohorts is needed, these results represent a step toward the development of imaging biomarkers to support differential diagnosis and prognostic assessment in FTD.

Author Contributions

Edoardo Gioele Spinelli: investigation, formal analysis, writing – review and editing, writing – original draft, data curation. **Francesca Orlandi:** writing – original draft, writing – review and editing, investigation. **Silvia Basaia:** investigation, writing – review and editing, formal analysis, data curation. **Francesco Costa:** writing – review and editing, investigation. **Stefano Pisano:** investigation, writing – review and editing, formal analysis. **Alma Ghirelli:** investigation, writing – review and editing, formal analysis. **Elisa Canu:** investigation, writing – review and editing, formal analysis. **Veronica Castelnovo:** investigation, writing – review and editing, formal analysis. **Elisa Sibilla:** investigation, writing – review and editing, formal analysis. **Giordano Cecchetti:** investigation, writing – review and editing. **Francesca Caso:** investigation, writing – review and editing. **Giuseppe Magnani:** investigation, writing – review and editing. **Paola Caroppo:** investigation, writing – review and editing, formal analysis. **Sara Prioni:** investigation, writing – review and editing, formal analysis. **Cristina Villa:** investigation, writing – review and editing, formal analysis. **Lucio Tremolizzo:** investigation, writing – review and editing, formal analysis. **Ildebrando Appollonio:** investigation, writing – review and editing, formal analysis. **Federico Verde:** investigation, writing – review and editing, formal analysis. **Nicola Ticozzi:** investigation, writing – review and editing, formal analysis. **Vincenzo Silani:** investigation, writing – review and editing, formal analysis. **Massimo Filippi:** conceptualization, writing – review and editing, supervision, formal analysis. **Federica Agosta:** conceptualization, writing – original draft, writing – review and editing, formal analysis, supervision.

Conflicts of Interest

E. G. Spinelli has nothing to disclose; F. Orlandi has nothing to disclose; S. Basaia receives research support from the Italian Ministry of Health; F. Costa has nothing to disclose; S. Pisano has nothing to disclose; A. Ghirelli has nothing to disclose; E. Canu receives research support from the Italian Ministry of Health; V. Castelnovo has nothing to disclose; E. Sibilla has nothing to disclose; G. Cecchetti has received speaker honoraria from Neopharmed Gentili; F. Caso has nothing to disclose; G. Magnani has nothing to disclose; P. Caroppo has nothing to disclose; S. Prioni has nothing to disclose; C. Villa has nothing to disclose; L. Tremolizzo has nothing to disclose; I. Appollonio has nothing to disclose; F. Vedre has nothing to disclose; N. Ticozzi is Associate Editor of Frontiers in Aging Neuroscience; he received compensation for consulting services and/or speaking activities from Biogen Italia, Zambon, Italfarmaco, and Amylyx Pharmaceuticals; he receives or has received research support from the Italian Ministry of Health and AriSLA; V. Silani is on the Editorial Board of Amyotrophic Lateral Sclerosis and Frontotemporal Degeneration, European Neurology, American Journal of Neurodegenerative Diseases, Frontiers in Neurology, and Exploration of Neuroprotective Therapy; he received compensation for consulting services and/or speaking activities from AveXis, Cytokinetics, Italfarmaco, Liquidweb S.r.l., Novartis Pharma AG, and Zambon; he receives or has received research support from the Italian Ministry of Health, AriSLA, and E-Rare Joint Transnational Call. M. Filippi is Editor-in-Chief of the Journal of Neurology, Associate Editor of Human Brain Mapping, Neurological Sciences, and Radiology; he received compensation for consulting services from Alexion, Almirall, Biogen, Merck, Novartis, Roche, Sanofi, speaking activities from Bayer, Biogen, Celgene, Chiesi Italia Spa, Eli Lilly, Genzyme, Janssen, Merck-Serono, Neopharmed Gentili, Novartis, Novo Nordisk, Roche, Sanofi, Takeda, and TEVA; participation in Advisory Boards for Alexion, Biogen, Bristol-Myers Squibb, Merck, Novartis, Roche, Sanofi, Sanofi-Aventis, Sanofi-Genzyme, Takeda; scientific direction of educational events for Biogen, Merck, Roche, Celgene, Bristol-Myers Squibb, Lilly, Novartis, Sanofi-Genzyme; he receives research

support from Biogen Idec, Merck-Serono, Novartis, Roche, the Italian Ministry of Health, the Italian Ministry of University and Research, and Fondazione Italiana Sclerosi Multipla; F. Agosta is an Associate Editor of NeuroImage: Clinical—has received speaker honoraria from Biogen Idec, Italfarmaco, Roche, Zambon, and Eli Lilly; he receives or has received research support from the Italian Ministry of Health, the Italian Ministry of University and Research, AriSLA (Fondazione Italiana di Ricerca per la SLA), the European Research Council, the EU Joint Programme—Neurodegenerative Disease Research (JPND), and Foundation Research on Alzheimer Disease (France).

Data Availability Statement

The dataset used and analyzed during the current study will be made available by the corresponding author upon request to qualified researchers (i.e., affiliated to a university or research institution/hospital).

References

1. M. Grossman, W. W. Seeley, A. L. Boxer, et al., "Frontotemporal Lobar Degeneration," *Nature Reviews. Disease Primers* 9, no. 1 (2023): 40, https://doi.org/10.1038/s41572-023-00447-0.

2. H. Ulugut and Y. A. L. Pijnenburg, "Frontotemporal Dementia: Past, Present, and Future," *Alzheimer's & Dementia* 19, no. 11 (2023): 5253–5263, https://doi.org/10.1002/alz.13363.

3. M. Filippi and F. Agosta, "MRI of Non-Alzheimer's Dementia: Current and Emerging Knowledge," *Current Opinion in Neurology* 31, no. 4 (2018): 405–414, https://doi.org/10.1097/wco.0000000000000571.

4. M. L. Gorno-Tempini, A. E. Hillis, S. Weintraub, et al., "Classification of Primary Progressive Aphasia and Its Variants," *Neurology* 76, no. 11 (2011): 1006–1014, https://doi.org/10.1212/WNL.0b013e31821103e6.

5. K. Rascovsky, J. R. Hodges, D. Knopman, et al., "Sensitivity of Revised Diagnostic Criteria for the Behavioural Variant of Frontotemporal Dementia," *Brain* 134, no. Pt 9 (2011): 2456–2477, https://doi.org/10.1093/brain/awr179.

6. H. Ulugut, M. Bertoux, K. Younes, et al., "Clinical Recognition of Frontotemporal Dementia With Right Anterior Temporal Predominance: A Multicenter Retrospective Cohort Study," *Alzheimer's & Dementia* 20, no. 8 (2024): 5647–5661, https://doi.org/10.1002/alz.14076.

7. A. Ghirelli, E. G. Spinelli, E. Canu, et al., "Clinical and Neuroanatomical Characterization of the Semantic Behavioral Variant of Frontotemporal Dementia in a Multicenter Italian Cohort," *Journal of Neurology* 271, no. 7 (2024): 4203–4215, https://doi.org/10.1007/s00415-024-12338-9.

8. K. Younes, V. Borghesani, M. Montembeault, et al., "Right Temporal Degeneration and Socioemotional Semantics: Semantic Behavioural Variant Frontotemporal Dementia," *Brain* 145, no. 11 (2022): 4080–4096, https://doi.org/10.1093/brain/awac217.

9. R. Santangelo, A. Dell'Edera, A. Sala, et al., "The CSF p-tau181/Aβ42 Ratio Offers a Good Accuracy "In Vivo" in the Differential Diagnosis of Alzheimer's Dementia," *Current Alzheimer Research* 16, no. 7 (2019): 587–595, https://doi.org/10.2174/1567205016666190725150836.

10. F. Agosta, E. G. Spinelli, S. Basaia, et al., "Functional Connectivity From Disease Epicenters in Frontotemporal Dementia," *Neurology* 100, no. 22 (2023): e2290–e2303, https://doi.org/10.1212/wnl.0000000000207277.

11. B. Fischl and A. M. Dale, "Measuring the Thickness of the Human Cerebral Cortex From Magnetic Resonance Images," *Proceedings of the National Academy of Sciences of the United States of America* 97, no. 20 (2000): 11050–11055, https://doi.org/10.1073/pnas.200033797.

12. M. Reuter, N. J. Schmansky, H. D. Rosas, and B. Fischl, "Within-Subject Template Estimation for Unbiased Longitudinal Image Analysis," *NeuroImage* 61, no. 4 (2012): 1402–1418, https://doi.org/10.1016/j.neuroimage.2012.02.084.

13. B. Patenaude, S. M. Smith, D. N. Kennedy, and M. Jenkinson, "A Bayesian Model of Shape and Appearance for Subcortical Brain Segmentation," *NeuroImage* 56, no. 3 (2011): 907–922, https://doi.org/10.1016/j.neuroimage.2011.02.046.

14. M. J. Cardoso, M. Modat, R. Wolz, et al., "Geodesic Information Flows: Spatially-Variant Graphs and Their Application to Segmentation and Fusion," *IEEE Transactions on Medical Imaging* 34, no. 9 (2015): 1976–1988, https://doi.org/10.1109/tmi.2015.2418298.

15. J. Diedrichsen, J. H. Balsters, J. Flavell, E. Cussans, and N. Ramnani, "A Probabilistic MR Atlas of the Human Cerebellum," *NeuroImage* 46, no. 1 (2009): 39–46, https://doi.org/10.1016/j.neuroimage.2009.01.045.

16. J. Diedrichsen, S. Maderwald, M. Küper, et al., "Imaging the Deep Cerebellar Nuclei: A Probabilistic Atlas and Normalization Procedure," *NeuroImage* 54, no. 3 (2011): 1786–1794, https://doi.org/10.1016/j.neuroimage.2010.10.035.

17. S. M. Smith, Y. Zhang, M. Jenkinson, et al., "Accurate, Robust, and Automated Longitudinal and Cross-Sectional Brain Change Analysis," *NeuroImage* 17, no. 1 (2002): 479–489, https://doi.org/10.1006/nimg.2002.1040.

18. A. Pérez-Millan, J. Contador, J. Juncà-Parella, et al., "Classifying Alzheimer's Disease and Frontotemporal Dementia Using Machine Learning With Cross-Sectional and Longitudinal Magnetic Resonance Imaging Data," *Human Brain Mapping* 44, no. 6 (2023): 2234–2244, https://doi.org/10.1002/hbm.26205.

19. P. L. Pan, W. Song, J. Yang, et al., "Gray Matter Atrophy in Behavioral Variant Frontotemporal Dementia: A Meta-Analysis of Voxel-Based Morphometry Studies," *Dementia and Geriatric Cognitive Disorders* 33, no. 2–3 (2012): 141–148, https://doi.org/10.1159/000338176.

20. A. Bejanin, G. Tammewar, G. Marx, et al., "Longitudinal Structural and Metabolic Changes in Frontotemporal Dementia," *Neurology* 95, no. 2 (2020): e140–e154, https://doi.org/10.1212/wnl.0000000000009760.

21. E. G. Spinelli, A. Ghirelli, S. Basaia, et al., "Structural MRI Signatures in Genetic Presentations of the Frontotemporal Dementia/Motor Neuron Disease Spectrum," *Neurology* 97, no. 16 (2021): e1594–e1607, https://doi.org/10.1212/wnl.0000000000012702.

22. T. W. Chow, A. Izenberg, M. A. Binns, et al., "Magnetic Resonance Imaging in Frontotemporal Dementia Shows Subcortical Atrophy," *Dementia and Geriatric Cognitive Disorders* 26, no. 1 (2008): 79–88, https://doi.org/10.1159/000144028.

23. J. C. Looi, O. Lindberg, B. B. Zandbelt, et al., "Caudate Nucleus Volumes in Frontotemporal Lobar Degeneration: Differential Atrophy in Subtypes," *AJNR. American Journal of Neuroradiology* 29, no. 8 (2008): 1537–1543, https://doi.org/10.3174/ajnr.A1168.

24. C. Möller, N. Dieleman, W. M. van der Flier, et al., "More Atrophy of Deep Gray Matter Structures in Frontotemporal Dementia Compared to Alzheimer's Disease," *Journal of Alzheimer's Disease* 44, no. 2 (2015): 635–647, https://doi.org/10.3233/jad-141230.

25. J. D. Rohrer, T. Lashley, J. M. Schott, et al., "Clinical and Neuroanatomical Signatures of Tissue Pathology in Frontotemporal Lobar Degeneration," *Brain* 134, no. Pt 9 (2011): 2565–2581, https://doi.org/10.1093/brain/awr198.

26. J. A. Collins, V. Montal, D. Hochberg, et al., "Focal Temporal Pole Atrophy and Network Degeneration in Semantic Variant Primary Progressive Aphasia," *Brain* 140, no. 2 (2017): 457–471, https://doi.org/10.1093/brain/aww313.

27. J. S. Snowden, J. M. Harris, J. C. Thompson, et al., "Semantic Dementia and the Left and Right Temporal Lobes," *Cortex* 107 (2018): 188–203, https://doi.org/10.1016/j.cortex.2017.08.024.

28. H. Ulugut Erkoyun, C. Groot, R. Heilbron, et al., "A Clinical-Radiological Framework of the Right Temporal Variant of Frontotemporal Dementia," *Brain* 143, no. 9 (2020): 2831–2843, https://doi.org/10.1093/brain/awaa225.

29. M. C. McKenna, R. H. Chipika, S. Li Hi Shing, et al., "Infratentorial Pathology in Frontotemporal Dementia: Cerebellar Grey and White Matter Alterations in FTD Phenotypes," *Journal of Neurology* 268, no. 12 (2021): 4687–4697, https://doi.org/10.1007/s00415-021-10575-w.

30. J. Kleinerova, M. Tahedl, M. C. McKenna, et al., "Cerebellar Dysfunction in Frontotemporal Dementia: Intra-Cerebellar Pathology and Cerebellar Network Degeneration," *Journal of Neurology* 272, no. 4 (2025): 289, https://doi.org/10.1007/s00415-025-13046-8.

31. J. L. Whitwell, V. M. Anderson, R. I. Scahill, M. N. Rossor, and N. C. Fox, "Longitudinal Patterns of Regional Change on Volumetric MRI in Frontotemporal Lobar Degeneration," *Dementia and Geriatric Cognitive Disorders* 17, no. 4 (2004): 307–310, https://doi.org/10.1159/000077160.

32. H. Ulugut, A. A. Dijkstra, M. Scarioni, et al., "Right Temporal Variant Frontotemporal Dementia Is Pathologically Heterogeneous: A Case-Series and a Systematic Review," *Acta Neuropathologica Communications* 9, no. 1 (2021): 131, https://doi.org/10.1186/s40478-021-01229-z.

33. E. G. Spinelli, M. L. Mandelli, Z. A. Miller, et al., "Typical and Atypical Pathology in Primary Progressive Aphasia Variants," *Annals of Neurology* 81, no. 3 (2017): 430–443, https://doi.org/10.1002/ana.24885.

34. W. W. Seeley, R. Crawford, K. Rascovsky, et al., "Frontal Paralimbic Network Atrophy in Very Mild Behavioral Variant Frontotemporal Dementia," *Archives of Neurology* 65, no. 2 (2008): 249–255, https://doi.org/10.1001/archneurol.2007.38.

35. J. P. Kim, J. Kim, Y. H. Park, et al., "Machine Learning Based Hierarchical Classification of Frontotemporal Dementia and Alzheimer's Disease," *NeuroImage: Clinical* 23 (2019): 101811, https://doi.org/10.1016/j.nicl.2019.101811.

36. W. W. Seeley, R. K. Crawford, J. Zhou, B. L. Miller, and M. D. Greicius, "Neurodegenerative Diseases Target Large-Scale Human Brain Networks," *Neuron* 62, no. 1 (2009): 42–52, https://doi.org/10.1016/j.neuron.2009.03.024.

37. J. Zhou, E. D. Gennatas, J. H. Kramer, B. L. Miller, and W. W. Seeley, "Predicting Regional Neurodegeneration From the Healthy Brain Functional Connectome," *Neuron* 73, no. 6 (2012): 1216–1227, https://doi.org/10.1016/j.neuron.2012.03.004.

38. M. C. McKenna, S. Li Hi Shing, A. Murad, et al., "Focal Thalamus Pathology in Frontotemporal Dementia: Phenotype-Associated Thalamic Profiles," *Journal of the Neurological Sciences* 436 (2022): 120221, https://doi.org/10.1016/j.jns.2022.120221.

39. M. Tahedl, E. L. Tan, R. H. Chipika, et al., "The Involvement of Language-Associated Networks, Tracts, and Cortical Regions in Frontotemporal Dementia and Amyotrophic Lateral Sclerosis: Structural and Functional Alterations," *Brain and Behavior: A Cognitive Neuroscience Perspective* 13, no. 11 (2023): e3250, https://doi.org/10.1002/brb3.3250.

Supporting Information

Additional supporting information can be found online in the Supporting Information section.